Variational perturbation theory for dynamic polarizabilities and dispersion coefficients

Wen Hao Xia,[1] Zhi Ling Zhou,[1] Li Guang Jiao,[1,2,3,*] Aihua Liu,[4] Henry E. Montgomery, Jr.,[5,†] Yew Kam Ho,[6] and Stephan Fritzsche[2,3,7]

[1]*College of Physics, Jilin University, Changchun 130012, People's Republic of China*
[2]*Helmholtz-Institut Jena, D-07743 Jena, Germany*
[3]*GSI Helmholtzzentrum für Schwerionenforschung GmbH, D-64291 Darmstadt, Germany*
[4]*Institute of Atomic and Molecular Physics, Jilin University, Changchun 130012, People's Republic of China*
[5]*Chemistry Program, Centre College, Danville, Kentucky 40422, USA*
[6]*Institute of Atomic and Molecular Sciences, Academia Sinica, Taipei 10617, Taiwan*
[7]*Theoretisch-Physikalisches Institut, Friedrich-Schiller-Universität Jena, D-07743 Jena, Germany*

(Received 4 July 2023; accepted 28 August 2023; published 14 September 2023)

An efficient method based on the variational perturbation theory (VPT) is proposed to conveniently calculate the atomic real- and imaginary-frequency dynamic polarizabilities and the interatomic dispersion coefficients. The developed method holds the great advantage that only the system ground state wave function and corresponding radial mean values are needed. Verification of the VPT method on one- and two-electron atoms indicates that the present approximation shows good agreement with calculations based on the sophisticated sum-over-states method. We apply the VPT method to examine the approximate Z-scaling laws of polarizabilities and dispersion coefficients in the He isoelectronic sequence, and to investigate the plasma screening effect on these quantities for embedded atoms. Our calculation demonstrates very well that the VPT method is capable of producing reasonably accurate static and dynamic polarizabilities as well as two- and three-atom dispersion coefficients for plasma-embedded atoms in a wide range of screening parameters.

DOI: 10.1103/PhysRevE.108.035305

I. INTRODUCTION

The standard method to calculate polarizability is built upon the perturbation theory, where the second-order correction to energy originating from the dipole interaction between an atom and external electric field scales quadratically to the field strength, with the coefficient being defined as half of the polarizability [1–4]. Perhaps the most extensively used method for calculating polarizabilities of atomic systems employs the so-called sum-over-states technique [2,3]. In these calculations, one generally needs the initial ground state of the system prepared with high quality, a complete set of final states covering both the discrete bound and continuum spectra, and accurate calculations of all related transition oscillator strengths. Such a method, although it produces quite reliable and accurate polarizabilities for general atomic systems, is nevertheless subject to low efficiency and requires significant computational effort.

An alternative and actually earlier developed method is based on the Hylleraas variational perturbation theory (VPT). The prototype of this method can be traced back to the pioneering work of Kirkwood [5] and Buckingham [6], where the static polarizability of an atom can be approximated utilizing only the ground state wave function and corresponding radial quantities. Dalgarno [1] demonstrated that the VPT method gives a rigorous lower bound to polarizability and can also be reformulated from the Hylleraas variational method [7]. A thorough review of the earlier development of the VPT method and its reconstruction based on the Linderberg inequality are available in the work by Montgomery and Pupyshev [8]. Some recent interest in applying the VPT method has been focused on, e.g., the variation of dipole polarizabilities in spatially confined atoms [8–12].

The dynamic polarizabilities, with either real or imaginary photon frequencies, have attracted more interest in recent years due to both their fundamental importance and practical applications. The real-frequency dynamic polarizabilities are closely related to quantities like tune-out and magic wavelengths, which play important roles in developing new atomic clocks [3,13–16]. The imaginary-frequency dynamic polarizabilities find their usefulness in the calculation of dispersion coefficients for the long-range van der Waals interactions between two or among many atoms [3,17–20]. The Hylleraas VPT method, although it has been well established for static polarizability, has not been suitably adapted for frequency-dependent dynamic polarizabilities. On the other hand, there is an increasing need for a large amount of and efficient calculations of polarizabilities, both static and dynamic, as well as interatomic dispersion coefficients for, e.g., highly charged isoelectronic sequences [21–25] and atoms or ions embedded in different plasma screening environments [26–36]. The purpose of the present work is to develop the VPT method to calculate frequency-dependent dynamic polarizabilities and interatomic dispersion coefficients, so as to provide a simple,

*lgjiao@jlu.edu.cn
†ed.montgomery@centre.edu

efficient, and yet reasonably accurate method to approach such a task.

This paper is organized as follows. The basic knowledge of the VPT method and the present extension of the method to dynamic polarizabilities and dispersion coefficients are described in Secs. II A and II B, respectively, followed by the compact expressions for one- and two-electron atoms in Sec. II C. Section III presents our detailed test on the static and dynamic polarizabilities as well as on the two- and three-atom dispersion coefficients for the H atom, He atom, He-like ions, and plasma-screened atoms. We summarize the present work in Sec. IV. Atomic units (a.u.) are used throughout this paper. The polarizability has the dimension of volume in a.u., and numerical values presented in this work are in units of a_0^3 where a_0 is the Bohr radius.

II. VARIATIONAL PERTURBATION THEORY

A. Static dipole polarizability

The static dipole polarizability of an N-electron atom can be expressed in the sum-over-states formalism [3] as

$$\alpha = 2\sum_{j\neq 0}\frac{\langle\Phi_0|z|\Phi_j\rangle\langle\Phi_j|z|\Phi_0\rangle}{E_j - E_0}, \tag{1}$$

where Φ_0 is the ground state wave function, $z = \sum_{q=1}^{N} z_q$ represents the z component of the electric dipole transition operator for an N-electron system, and $\{\Phi_j\}$ are the complete orthonormalized set of the eigenfunctions of the system Hamiltonian with eigenenergies $\{E_j\}$. By defining the orthogonal projection operator

$$P_0 = 1 - |\Phi_0\rangle\langle\Phi_0| = \sum_{j\neq 0}|\Phi_j\rangle\langle\Phi_j|, \tag{2}$$

the static dipole polarizability can be formally written as

$$\alpha = 2\langle\Phi_0|zP_0(H - E_0)^{-1}P_0z|\Phi_0\rangle. \tag{3}$$

The fundamental idea of applying the Hylleraas VPT method for polarizability is to reexpand the subspace spanned by $\{\Phi_j\}_{(j\neq 0)}$ in terms of a simplified k-dimensional basis set

$$\zeta_j = P_0\xi_j \quad (j = 1, \ldots, k), \tag{4}$$

where P_0 is defined by Eq. (2) and the ξ_j must be some functions from the domain of definition of the Hamiltonian having the same symmetry as $z\Phi_0$. The goodness of the VPT approximation depends closely upon the choice of the basis functions ξ_j. Perhaps the simplest and also the most easily applicable form is [8,12]

$$\xi_j = \sum_{p=1}^{N} z_p r_p^{j-1}\Phi_0, \tag{5}$$

in which r_p is the distance from the origin to the pth electron and z_p is the corresponding z component.

Performing the spectral decomposition of the Hamiltonian operator in Eq. (3) based on the new k-dimensional basis set $\{\zeta_j\}_{(j=1-k)}$, the integral calculation of the dipole polarizability is then reduced to the matrix multiplications in the form

$$\alpha = 2[\mathbf{B}]^{\dagger}[\mathbf{D}]^{-1}[\mathbf{B}], \tag{6}$$

where the column vector $[\mathbf{B}]$ is composed of elements

$$B_j = \langle\zeta_j|z|\Phi_0\rangle \equiv \langle\xi_j|P_0z|\Phi_0\rangle, \tag{7}$$

and the Hamiltonian matrix $[\mathbf{D}]$ has the elements

$$D_{ij} = \langle\zeta_i|H - E_0|\zeta_j\rangle \equiv \langle\xi_i|H - E_0|\xi_j\rangle. \tag{8}$$

Substituting Eq. (5) into Eqs. (7) and (8) and after some algebraic manipulations, we finally have

$$B_j = \frac{N(N+1)}{6}\langle r_p^{j+1}\rangle + \frac{1}{3}\sum_{p>q}\left[\langle r_p^2 r_q^{j-1}\rangle - \langle r_{pq}^2 r_q^{j-1}\rangle\right], \tag{9}$$

and

$$D_{ij} = \frac{N(2+ij)}{6}\langle r_p^{i+j-2}\rangle. \tag{10}$$

Here we have simplified the notation of ground state radial expectation values $\langle\Phi_0|f(r)|\Phi_0\rangle$ as $\langle f(r)\rangle$.

The great advantage of the Hylleraas VPT method for calculating dipole polarizability relies upon the fact that it depends only on the system ground state wave function and radial expectation values like $\langle r_1^n\rangle$, $\langle r_1^n r_2^2\rangle$, and $\langle r_1^n r_{12}^2\rangle$. Unlike the sophisticated sum-over-states formalism displayed in Eq. (1), where one generally needs to construct complete (both discrete bound and continuum) final excited states and calculate the corresponding transition oscillator strengths, the VPT method does not need any information about the excited states. Additionally, it has been strictly proved that the VPT method predicts a lower bound for the dipole polarizability [1,8] and the approximation approaches the exact quantity by gradually increasing the dimension of the basis set $\{\zeta_j\}$, i.e.,

$$\alpha^{k_1} \leqslant \alpha^{k_2} \leqslant \alpha \quad (k_1 \leqslant k_2). \tag{11}$$

For example, for $k = 1$ the VPT method was originally named Kirkwood's approximation [5],

$$\alpha_{\mathrm{K}} = 2\frac{B_1^2}{D_{11}}. \tag{12}$$

For $k = 2$, the VPT method is commonly known as Buckingham's approximation [6]

$$\alpha_{\mathrm{B}} = 2\frac{B_1^2 D_{22} - 2B_1B_2D_{12} + B_2^2D_{11}}{D_{11}D_{22} - D_{12}^2}. \tag{13}$$

It is therefore natural that

$$\alpha_{\mathrm{K}} \leqslant \alpha_{\mathrm{B}} \leqslant \alpha. \tag{14}$$

B. Dynamic polarizability and dispersion coefficients

The extension of the Hylleraas VPT method to dynamic polarizability is not that straightforward if one starts from the matrix multiplication form of Eq. (6). The sum-over-states formalism for the dynamic polarizability [3] reads

$$\alpha(\omega) = 2\sum_{j\neq 0}\frac{(E_j - E_0)\langle\Phi_0|z|\Phi_j\rangle\langle\Phi_j|z|\Phi_0\rangle}{(E_j - E_0)^2 - \omega^2}, \tag{15}$$

where ω is the photon frequency. Following a similar procedure as in Eq. (3), the formal expression for dynamic

polarizability is given by

$$\begin{aligned}\alpha(\omega) &= 2\langle\Phi_0|zP_0\frac{H-E_0}{(H-E_0)^2-\omega^2}P_0z|\Phi_0\rangle \\ &= 2\langle\Phi_0|zP_0(H-E_0+\omega)^{-1}(H-E_0) \\ &\quad\times(H-E_0-\omega)^{-1}P_0z|\Phi_0\rangle, \end{aligned} \tag{16}$$

where the Hamiltonian operators $(H-E_0+\omega)^{-1}$, $(H-E_0)$, and $(H-E_0-\omega)^{-1}$ commute with each other. Applying the spectral decomposition to all three Hamiltonian operators based on the k-dimensional basis set $\{\zeta_j\}_{(j=1-k)}$ results in

$$\alpha(\omega) = 2[\mathbf{B}]^{\dagger}[\mathbf{D}^{+}]^{-1}[\mathbf{D}][\mathbf{D}^{-}]^{-1}[\mathbf{B}], \tag{17}$$

where

$$D_{ij}^{+} = D_{ij} + W_{ij}, \tag{18}$$

$$D_{ij}^{-} = D_{ij} - W_{ij}, \tag{19}$$

and

$$W_{ij} = \omega\langle\zeta_i|\zeta_j\rangle \equiv \omega\langle\xi_i|\xi_j\rangle. \tag{20}$$

The elements in column vector [**B**] and Hamiltonian matrix [**D**] are given by Eqs. (7) and (8), respectively.

For the special choice of the basis function in Eq. (5), the overlap matrix element is obtained as

$$\langle\xi_i|\xi_j\rangle = \frac{N}{3}\langle r_p^{i+j}\rangle + \frac{1}{3}\sum_{p>q}\langle(\vec{r}_p\cdot\vec{r}_q)\big(r_p^{i-1}r_q^{j-1}+r_p^{j-1}r_q^{i-1}\big)\rangle, \tag{21}$$

where the vector term $\vec{r}_p\cdot\vec{r}_q$ can be easily transformed into scalar products of radial variables through the cosine law

$$\vec{r}_p\cdot\vec{r}_q = \tfrac{1}{2}\big(r_p^2+r_q^2-r_{pq}^2\big). \tag{22}$$

From Eq. (17) it can be readily observed that the application of Hylleraas VPT method to dynamic polarizability has the same advantage as it does for static polarizability, i.e., the calculation depends only on the ground state wave function and the corresponding radial expectation values.

The imaginary-frequency dynamic polarizability $\alpha(i\omega)$ somehow attracts more interest in the literature due to its close relationship with the dispersion coefficients in constructing the van der Waals potential among atoms [17–20]. For a pair of atoms (a and b), the long-range interaction can be expressed as

$$V_{ab} = -\frac{C_6}{R_{ab}^6} - O\big(R_{ab}^{-8}\big) - \cdots, \tag{23}$$

where the dispersion coefficient C_6 comes from the instantaneous dipole-dipole interaction and is defined by

$$C_6 = \frac{3}{\pi}\int_0^{\infty}\alpha_a(i\omega)\alpha_b(i\omega)d\omega. \tag{24}$$

The leading term of the nonadditive long-range interaction for a three-atom system is given by

$$V_{abc} = -\frac{C_9}{R_{ab}^3R_{bc}^3R_{ac}^3}(3\cos\theta_a\cos\theta_b\cos\theta_c+1) - \cdots, \tag{25}$$

where the dispersion coefficient C_9 (which is also usually named as Z_{111} [19]) comes from the triple-dipole interaction among three atoms:

$$C_9 = \frac{3}{\pi}\int_0^{\infty}\alpha_a(i\omega)\alpha_b(i\omega)\alpha_c(i\omega)d\omega. \tag{26}$$

Accurate calculation of the dispersion coefficients provides an alternative estimate of the accuracy of dynamic polarizabilities in the entire range of photon frequency. Extension of the VPT method to imaginary-frequency dynamic polarizability $\alpha(i\omega)$ and the subsequent dispersion coefficients is quite straightforward by replacing ω in Eq. (20) by $i\omega$, where the only price to pay is the inversion of complex matrices $[\mathbf{D}^{+}]$ and $[\mathbf{D}^{-}]$.

C. One- and two-electron atoms

While the above derivation can be performed for general N-electron systems, the computational procedure and matrix elements can be greatly simplified for one- and two-electron atoms. For these simple systems, analytical or accurate numerical predictions of static and dynamic polarizabilities as well as dispersion coefficients are available in the literature for benchmark comparison.

For one-electron atoms, where all interelectronic radii disappear, the matrix elements reduce to

$$B_j = \frac{1}{3}\langle r^{j+1}\rangle, \tag{27}$$

$$D_{ij} = \frac{2+ij}{6}\langle r^{i+j-2}\rangle, \tag{28}$$

$$W_{ij} = \frac{\omega}{3}\langle r^{i+j}\rangle. \tag{29}$$

For two-electron atoms, i.e., $N=2$, we finally have

$$B_j = \frac{2}{3}\big[\langle r_1^{j+1}\rangle + \langle(\vec{r}_1\cdot\vec{r}_2)r_1^{j-1}\rangle\big], \tag{30}$$

$$D_{ij} = \frac{2+ij}{3}\langle r_1^{i+j-2}\rangle, \tag{31}$$

$$W_{ij} = \frac{\omega}{3}\big[2\langle r_1^{i+j}\rangle + \langle(\vec{r}_1\cdot\vec{r}_2)\big(r_1^{i-1}r_2^{j-1}+r_1^{j-1}r_2^{i-1}\big)\rangle\big]. \tag{32}$$

III. RESULTS AND DISCUSSION

A. H atom

The static dipole polarizability of the ground state of the H atom is analytically available as $\alpha = 4.5$ and therefore can be utilized as a convergence test to the present method. It is known that the radial expectation values of the ground state of the H atom read [37]

$$\langle r^n\rangle = \frac{(n+2)!}{2^{n+1}}. \tag{33}$$

The use of $k=1$ in Eq. (6) gives $\alpha = 4.0$, and for any values of $k \geqslant 2$ the VPT method surprisingly predicts the exact dipole polarizability of $\alpha = 4.5$.

The real-frequency dynamic polarizabilities $\alpha(\omega)$, however, show slower convergence than that for the static polarizability. We show in Fig. 1 the variation of $\alpha(\omega)$ for the ground state of the H atom with the basis-set dimensions $k = 2$, 5, and 25, together with comparison with the accurate

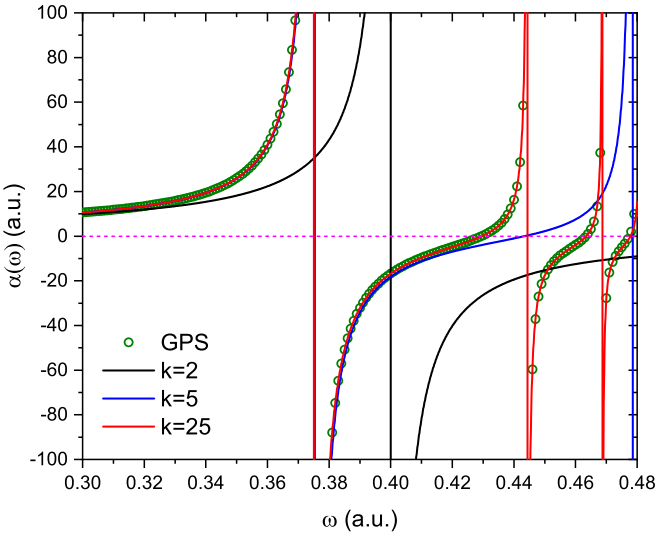

FIG. 1. Real-frequency dynamic polarizability $\alpha(\omega)$ for the ground state of the H atom. Solid lines represent the present VPT approximations with $k = 2$, 5, and 25. Dots are the sum-over-states calculations based on the GPS method [38].

sum-over-states calculations based on the generalized pseudospectral (GPS) method [38]. The GPS method has been well established in the literature to numerically solve the radial Schrödinger equation in the discrete variable representation [40–42]. In our previous work, we successfully applied the GPS method to produce highly accurate dipole polarizability and hyperpolarizability for one-electron systems [38,43,44]. The dynamic polarizabilities based on the GPS method also show very good agreement with the recent work of Wang *et al.* [39] using the Slater-type-orbital expansions. Therefore, for one-electron atoms the GPS numerical calculations of dynamic polarizability using the sum-over-states formalism can be considered as benchmark results for comparison.

The real-frequency dynamic polarizabilities manifest two distinct features with gradual increase of the photon frequency from zero [where $\alpha(0) = \alpha$] to the ground state ionization energy ($\omega_{\text{ionization}}^{\text{H}(1s)} = 0.5$). At resonant frequencies the dynamic polarizability makes a jump from positive to negative infinity due to the appearance of a singularity in the denominator of Eq. (15), i.e., $\omega_r = E_j - E_0$. Therefore, the resonant frequencies ideally indicate the transition energies between the ground and the dipole-allowed excited states. The tune-out photon frequencies, on the other hand, are defined at the positions where dynamic polarizability disappears, i.e., $\alpha(\omega_t)$=0. For external electric fields with these special frequencies, the target atoms do not produce energy shifts (except for the higher-order effects).

Besides the comparison displayed in Fig. 1, we also show in Table I the VPT predictions of the first three resonant and tune-out frequencies for $k = 1$ to 25. It is clearly seen that for small values of k, although the dynamic polarizability successfully reproduces the static polarizability at $\omega = 0$, both the number and position of the predicted resonant and tune-out frequencies are far from the analytic values of $\omega_{ri} = 1/2 - 1/[2(i+1)^2]$ and accurate numerical calculations of ω_{ti} from Wang *et al.* [39]. The use of $k = 2$ only predicts a single resonant frequency at $\omega_{r1} = 0.400$ and $k = 5$ the first tune-out frequency at $\omega_{t1} = 0.4434$. The convergence for both ω_r and ω_t improves significantly as the basis-set dimension k increases, with the lower-frequency quantities converging faster than higher-frequency quantities. Recalling from Eq. (4) that the k-dimensional basis set $\{\zeta_j\}_{(j=1-k)}$ should ideally cover the entire subspace spanned by $\{\Phi_j\}_{(j\neq 0)}$ and remembering the fact that the number of p-wave states in the H atom is infinitely large, it is not surprising that one generally needs to increase k so as to approach the exact dynamical polarizabilities in the entire range of photon frequencies. If, however, we are only interested in the low-frequency dynamic polarizabilities below the first resonant frequency, the use of small values of k in the VPT method is fully capable of producing accurate predictions. Taking Fig. 1 as an example, the calculations with $k = 5$ are already in good agreement with the referenced values for $\omega < 0.42$.

TABLE I. The first three resonant photon frequencies (ω_{r1}, ω_{r2}, ω_{r3}) and tune-out photon frequencies (ω_{t1}, ω_{t2}, ω_{t3}) for the dynamic polarizability of the ground state of the H atom predicted by the VPT method at different values of k. "A" represents the analytic values of $\omega_{ri} = 1/2 - 1/[2(i+1)^2]$ and the accurate calculations of ω_{ti} by Wang *et al.* [39].

k	ω_{r1}	ω_{t1}	ω_{r2}	ω_{t2}	ω_{r3}	ω_{t3}
1	0.5000					
2	0.4000					
3	0.3811					
4	0.3765	0.4646				
5	0.3754	0.4434	0.4786			
6	0.3751	0.4353	0.4611			
7	0.3751	0.4319	0.4527			
8	0.3750	0.4305	0.4485	0.4930		
9	0.3750	0.4299	0.4464	0.4813	0.4994	
10	0.3750	0.4297	0.4454	0.4743	0.4888	
12	0.3750	0.4296	0.4446	0.4674	0.4774	
14	0.3750	0.4295	0.4445	0.4648	0.4723	0.4945
16	0.3750	0.4295	0.4445	0.4639	0.4702	0.4865
18	0.3750	0.4295	0.4444	0.4636	0.4693	0.4822
20	0.3750	0.4295	0.4444	0.4635	0.4689	0.4799
22	0.3750	0.4295	0.4444	0.4634	0.4688	0.4786
25	0.3750	0.4295	0.4444	0.4634	0.4688	0.4778
A	0.3750	0.4295[a]	0.4444	0.4634[a]	0.4688	0.4775[a]

[a]Wang *et al.* [39]

The imaginary-frequency dynamic polarizabilities $\alpha(i\omega)$ calculated by applying the VPT method are displayed in Fig. 2. It is surprisingly found that the use of only $k = 2$ is capable of producing very good agreement with the benchmark GPS sum-over-states calculations. The results using larger values of k are indistinguishable from those with $k = 2$ in the present figure scale. All VPT approximations with $k \geqslant 2$ are slightly smaller than the referenced values at high frequencies. However, such underestimation does not lead to significant discrepancies due to the fast decrease of $\alpha(i\omega)$ with increasing ω.

By integrating Eqs. (24) and (26), we are able to estimate the two- and three-atom dispersion coefficients among the H atoms. Our calculated results at different values of k are shown

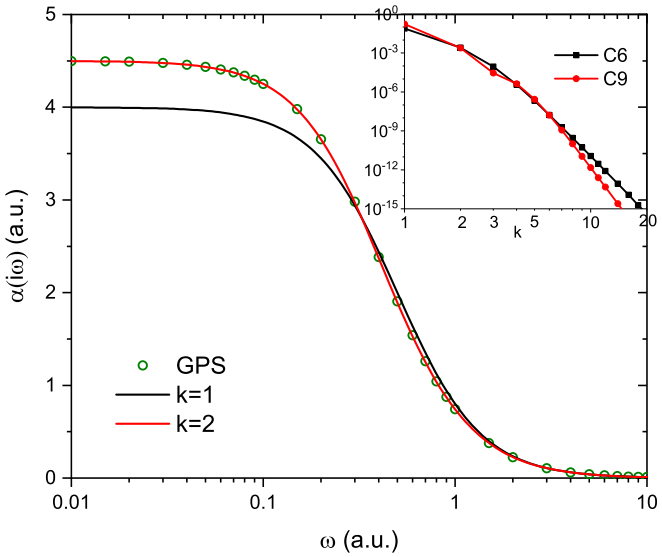

FIG. 2. Imaginary-frequency dynamic polarizability $\alpha(i\omega)$ for the ground state of the H atom. Solid lines represent the present VPT approximations with $k = 1$ and 2. Dots are the sum-over-states calculations based on the GPS method [38]. The inset shows the relative errors of dispersion coefficients C_6 and C_9 as a function of k on a logarithmic scale.

in Table II and compared with the most accurate predictions of Yan *et al.* [18] available in the literature. It is anticipated from the good agreement in Fig. 2 that the quantities C_6 and C_9 obtained by the VPT approximation with $k = 2$ are quite satisfactory, considering the simplicity of the present method. The convergence of calculations can be easily improved by gradually increasing k, as shown in the inset of Fig. 2, with the three-atom coefficient converging even faster than the two-atom coefficient. This is probably because the integrand of the dispersion coefficient C_9 is composed of three dynamic polarizabilities and therefore depends less on the high-frequency component compared to C_6. By employing $k = 20$, we finally arrive at the dispersion coefficients of C_6 and C_9 with an accuracy close to the double-precision limit.

TABLE II. The static dipole polarizability α, two-atom dispersion coefficient C_6, and three-atom dispersion coefficient C_9 for the ground state of the H atom predicted by the VPT method at different values of k. "A" represents the accurate calculations of C_6 and C_9 by Yan *et al.* [18].

k	α	C_6	C_9
1	4.0	6.0	18.0
2	4.5	6.482142857142859	21.59024234693878
3	4.5	6.498443983402488	21.64308331252906
4	4.5	6.499002577446928	21.64255727701200
5	4.5	6.499025354924765	21.64247042614076
6	4.5	6.499026596235598	21.64246486944496
7	4.5	6.499026692979891	21.64246453554672
8	4.5	6.499026703545927	21.64246451279089
9	4.5	6.499026705061502	21.64246451087294
10	4.5	6.499026705330400	21.64246451066844
12	4.5	6.499026705400507	21.64246451063702
14	4.5	6.499026705405283	21.64246451063603
16	4.5	6.499026705405762	21.64246451063598
18	4.5	6.499026705405827	21.64246451063597
20	4.5	6.499026705405837	21.64246451063597
A	4.5	6.499026705405839[a]	21.64246451063597[a]

[a]Yan *et al.* [18]

B. He atom

The He atom is one of the simplest many-electron systems that include electron correlation. To investigate the applicability and convergence of the VPT method for the He atom, we consider two types of wave function for the initial ground state, namely the configuration-interaction function based on Slater-type orbitals (STOCI) [48] and the explicitly correlated Hylleraas configuration-interaction function (HyCI) [49–52]. Both of these two types of wave function can be uniformly expressed as

$$\Phi_0(\vec{r}_1,\vec{r}_2) = \hat{A}\sum_{k=0}^{k_{\max}}\sum_{l_{a,b}=0}^{l_{\max}}\sum_{i,j} C_{a_i,b_j} r_{12}^k \phi_{a_i}(r_1)\phi_{b_j}(r_2) \times Y_{l_a,l_b}^{LM}(\hat{r}_1,\hat{r}_2) S^{S,M_S}(\sigma_1,\sigma_2), \tag{34}$$

where $\hat{A}$ is the antisymmetric operator, $Y_{l_a,l_b}^{LM}(\hat{r}_1,\hat{r}_2)$ and $S^{S,M_S}(\sigma_1,\sigma_2)$ are the two-electron coupled orbital angular momentum and spin wave functions, respectively. $\phi(r)$ is the radial part of the one-electron STO

$$\phi_a(r) = r^{n_a-1}e^{-\xi_a r}, \tag{35}$$

in which ξ is a nonlinear parameter to be determined in the variational calculation. For $k_{\max} = 0$, i.e., no r_{12} coordinate is included in the basis set, Eq. (34) reduces to the conventional STOCI basis set. $k_{\max} \geqslant 1$ corresponds to the explicitly correlated HyCI basis set. Here we generally set $k_{\max} = 1$, which gives a good balance between the completeness of the basis set and computational efficiency. The naming schemes for both the STOCI and HyCI basis sets are unified as $(n_1, n_2, \ldots)k_{\max}$, which means that we first use several groups of STOs to construct a near complete one-electron basis set, with each group of STOs having the largest principal quantum number n_i and all possible values of orbital angular momentum l_i ($< n_i$). The one-electron basis sets are then coupled to construct the two-electron basis set in the configuration-interaction manner.

The STOCI calculations of the He atom ground state energy, static dipole polarizability, and two- and three-atom dispersion coefficients are summarized in the top section of Table III. Here we choose (6,4,2)0, (7,5,3)0, and (8,6,4)0 basis sets, which couple to the total numbers of 158, 278, and 449 terms in the expansion of the ground state wave function. With gradual enlargement of the basis set, the relative error of energy δE_0 decreases from 7.6×10^{-5} to 3.0×10^{-5}. For a quantitative comparison of the quality of the initial wave function, we also include perhaps the most accurate CI calculation by Bromley and Mitroy [45,53] who employed 8586 terms of basis functions built upon the Laguerre-type orbitals and predicted the ground state energy with a relative error 4.0×10^{-6}. For the dipole polarizability and dispersion coefficients, we gradually increase the dimension k to make

TABLE III. The bound energy E_0, static dipole polarizability α, two-atom dispersion coefficient C_6, and three-atom dispersion coefficient C_9 for the ground state of the He atom predicted by the VPT method with $k = 15$ for different types of basis set. "LTOCI" represents the CI calculation of energy by Bromley and Mitroy [45] based on the Laguerre-type orbitals. "Hylleraas" refers to the benchmark predictions of α, C_6, and C_9 by Yan *et al.* [18] based on the Hylleraas wave function.

Basis	N_{basis}	E_0	δE_0	α	$\delta\alpha$	C_6	δC_6	C_9	δC_9
(6,4,2)0	158	−2.903503872	7.6[−5]	1.379179304	0.290%	1.458137817	0.194%	1.472877100	0.452%
(7,5,3)0	278	−2.903589433	4.6[−5]	1.379412517	0.273%	1.458378795	0.178%	1.473319819	0.422%
(8,6,4)0	449	−2.903635883	3.0[−5]	1.379454574	0.270%	1.458423728	0.175%	1.473397143	0.416%
LTOCI	8586	−2.903712786[a]	4.0[−6]						
(4,4)1	140	−2.903724371692	1.8[−9]	1.379488819	0.268%	1.458436737	0.174%	1.473418832	0.415%
(5,5)1	250	−2.903724376813	7.6[−11]	1.379493578	0.267%	1.458439337	0.174%	1.473424076	0.415%
(6,6)1	406	−2.903724377019	5.2[−12]	1.379493856	0.267%	1.458439474	0.174%	1.473424353	0.415%
Hylleraas		−2.903724377034[b]		1.383192174[c]		1.460977837[c]		1.479558606[c]	

[a]Bromley and Mitroy [45].
[b]Drake *et al.* [46].
[c]Yan *et al.* [18]; see also Pachucki and Sapirstein [47] for more accurate dipole polarizability.

sure that convergence under the VPT approximation is fully achieved. As demonstrated in Table IV, the use of $k = 15$ is responsible for all these quantities converging to the ninth digit after the decimal point. Actually, the use of k as small as 3 is good enough to produce results with three-digits accuracy.

From Table III we find that although the ground state energy (and wave function) has achieved a high accuracy and the VPT method has been fully converged, the calculations of α, C_6, and C_9 still differ to a comparably large extent from the accurate predictions of Yan *et al.* [18] using the sum-over-states method based on the Hylleraas basis functions [49]. To remove possible inaccuracy from the initial ground state wave function, we further performed the VPT calculations based on the (4,4)1, (5,5)1, and (6,6)1 HyCI basis sets. The accuracy of the ground state energies has been improved by several orders of magnitude using the HyCI basis sets; the predictions of α, C_6, and C_9, however, do not improve significantly.

The discrepancy between the present VPT calculations and the referenced results should be attributed to the incompleteness of the basis set $\{\zeta_j\}_{(j=1-k)}$, even in the limit of $k \to \infty$.

TABLE IV. Convergence of the static dipole polarizability α, two-atom dispersion coefficient C_6, and three-atom dispersion coefficient C_9 for the ground state of the He atom predicted by the VPT method at different values of k. The ground state wave function is represented by the (8,6,4)0 STOCI basis set.

k	α	C_6	C_9
1	1.132492802	1.278290133	1.085740781
2	1.379323401	1.451094986	1.467019982
3	1.379384550	1.458232609	1.473550014
4	1.379439574	1.458408733	1.473360361
5	1.379449487	1.458416604	1.473379557
6	1.379454047	1.458421945	1.473394278
7	1.379454519	1.458423516	1.473397045
8	1.379454534	1.458423699	1.473397087
10	1.379454546	1.458423714	1.473397108
12	1.379454557	1.458423720	1.473397123
14	1.379454572	1.458423728	1.473397143
15	1.379454574	1.458423728	1.473397143

This can be understood from Eq. (11), where a smaller basis set only predicts a lower bound of the exact polarizability. As a matter of fact, the simple form of Eq. (5) for the functions ξ_j employed in the present work is limited to the *one-electron excitation* component, which means that these functions are ideally complete ($k \to \infty$) only for one-electron atoms, while in many-electron atoms the multielectron excitations are necessary for a complete description of the subspace orthogonalized to the ground state. An alternative choice for the two-electron atom is

$$\xi_m = (z_1 + z_2) r_1^{i-1} r_2^{j-1} \Phi_0 \quad (i, j \geqslant 1), \tag{36}$$

where the multiple index m enumerates all possible combinations of (i, j). If the ground state wave function is expressed in terms of an explicitly correlated basis set such as the Hylleraas or HyCI type, the more accurate and efficient function can be [12]

$$\xi_m = (z_1 + z_2) r_1^{i-1} r_2^{j-1} r_{12}^{k-1} \Phi_0, \quad (i, j, k \geqslant 1), \tag{37}$$

where the index m enumerates all possible combinations of (i, j, k). The use of either Eq. (36) or (37) would, however, significantly increase the complexities in the expression of vector [**B**] and matrices [**D**] and [**W**] by radial expectation quantities. On the other hand, the extension of Eqs. (36) and (37) to general many-electron systems seems to be less competitive than the sophisticated sum-over-states method and obviously destroys the simplicity of the VPT method. Considering that the VPT method is not very sensitive to the ground state wave function and it produces fairly good estimates of the static and dynamic polarizabilities (e.g., $\delta\alpha < 0.3\%$ for the He atom) and the two- and three-atom dispersion coefficients ($\delta C_6 < 0.2\%$, $\delta C_9 < 0.5\%$), we restrict all our calculations in the present work based on Eq. (5), and would like to leave the application of Eqs. (36) and (37) as a future work.

Figure 3 displays the real-frequency dynamic polarizabilities $\alpha(\omega)$ for the ground state of the He atom calculated by the VPT method at different values of k. A brief summary of referenced values is given by Bishop and Pipin [54] and Kar [29]. The (8,6,4)0 STOCI basis set is used in the expansion of the ground state wave function. As in the H atom, the use of $k = 1$ does not produce any resonant

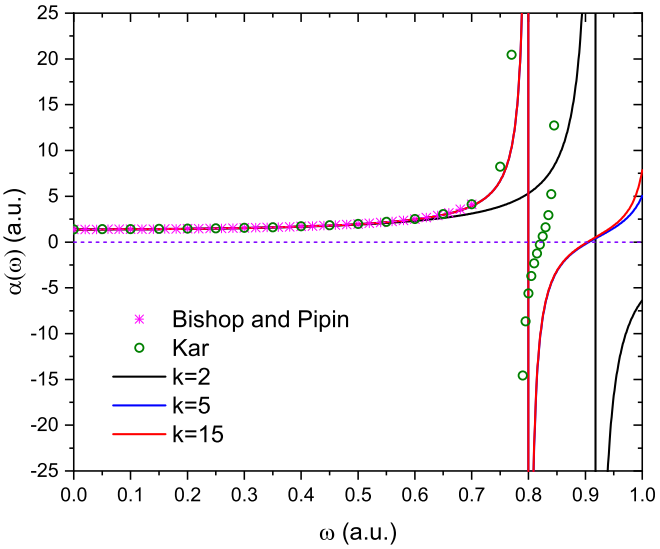

FIG. 3. Real-frequency dynamic polarizability $\alpha(\omega)$ for the ground state of the He atom. Solid lines represent the present VPT approximations with $k = 2$, 5, and 15. Dots are the sum-over-states calculations by Bishop and Pipin [54] and Kar [29].

photon frequencies below the ground state ionization energy ($\omega^{\rm He}_{\rm ionization} = 0.903724$). The use of $k = 2$ predicts the first resonant frequency at $\omega_{r1} = 0.917$, and both $k = 5$ and 15 give $\omega_{r1} = 0.799$, which is slightly larger than the exact value of $\omega_{r1} = E_1(^1P^o) - E_0(^1S^e) = 0.780$. The incorrect behavior of the dynamic polarizabilities above the first resonant frequency as well as the missing of higher-lying resonant frequencies are attributed to the *one-electron excitation* approximation inherent in the restrictive basis function of Eq. (5). Nevertheless, we conclude that the VPT method is capable of producing reliable estimates of the real-frequency dynamic polarizabilities below the first resonant frequency.

It is interesting to make a rough comparison of the computation time between the present VPT method and the usual sum-over-states method. For the dipole polarizability, if the dimension of the P-wave excited states is of the same order of magnitude as that of the ground S-wave state and the computation time for calculating each dipole transition matrix element is approximately equal to the time for each radial mean value, the speed-up factor of the VPT method compared to the sum-over-states method would roughly be the ratio between the dimension of the P-wave states and the total number of radial mean values calculated. Taking the He atom as an example, when the (8,6,4)0 STOCI basis set is used for constructing the singlet P-wave states ($N^P_{\rm basis} = 646$) and $k = 4$ is employed in the VPT method to converge the polarizability to the fourth digit ($\alpha = 1.3794$), the speed-up factor would probably be $N^P_{\rm basis}/(k^2 + 2k) \approx 27$, which means that the VPT method is more than 20 times faster than the sum-over-states method.

C. He-like ions

There exists a rigorous Z-scaling law for the dipole polarizabilities of one-electron atoms [38,58]. For the H-like ion with nuclear charge Z, it is

$$Z^4\alpha^{\rm H}(Z) = \alpha^{\rm H}(Z = 1). \tag{38}$$

The use of a similar law for dynamic polarizabilities yields the Z-scaling laws for the two- and three-atom dispersion coefficients (here we only focus on the homonuclear diatomic and triatomic systems)

$$Z^6C_6^{\rm H}(Z) = C_6^{\rm H}(Z = 1), \quad Z^{10}C_9^{\rm H}(Z) = C_9^{\rm H}(Z = 1). \tag{39}$$

Such Z-scaling laws, however, do not apply to many-electron atoms due to the existence of electron correlation.

Taking advantage of the simplicity and fast convergence (with respect to the dimension k) of the VPT method, we investigate the variation of dipole polarizability and the two- and three-atom dispersion coefficients for the He isoelectronic sequence. The (8,6,4)0 STOCI basis set is employed for all He-like ions from $Z = 2$ to 20, and the calculated results are summarized in Table V. For ions with $2 \leqslant Z \leqslant 10$, Zhu *et al.* [56] have performed the most accurate predictions of α and C_6 so far using the sum-over-states method based on the Hylleraas basis functions. Patil [57] estimated the three-atom dispersion coefficient C_9 for the He atom and Li^+ and Be^{2+} ions based on asymptotic two-electron wave functions. Their results are included in Table V for reference. It is not surprising that, with gradually increasing nuclear charge, the present calculations of ground state energy, dipole polarizability, and two-atom dispersion coefficient agree better with the referenced results. This is attributed to both a better description of the ground state wave function using the same basis set and a more complete description of the excited subspace, as the nuclear charge is increased. It is then a rather natural conjecture that as $Z \to \infty$, where the electron correlation disappears, some Z-scaling laws similar to Eqs. (38) and (39) should be applicable to the many-electron isoelectronic sequence.

The asymptotic behavior of dipole polarizabilities for isoelectronic sequences have been investigated by Koch and Andrae [21,22] in the framework of restricted Hartree-Fock theory. A more rigorous derivation of the approximate dipole polarizabilities for two-electron atoms was performed by Dalgarno and Stewart [59] and Drake and Cohen [60] using the $1/Z$ expansion technique. It was shown that for He-like ions with large values of Z, the leading term of the exact Z expression reads $\alpha = 9/(Z - 0.359375)^4$, where the coefficient 0.359375 in the denominator represents an average screening effect on one electron from the other in the two-electron atom [60]. The quantity 9 in the numerator can be understood as follows. The Hamiltonian of two-electron atoms can be transformed into a Z-scaled form [52],

$$\frac{H}{Z^2} = -\frac{1}{2}\nabla^2_{\rho_1} - \frac{1}{2}\nabla^2_{\rho_2} - \frac{1}{\rho_1} - \frac{1}{\rho_2} + \frac{1}{Z}\frac{1}{\rho_{12}}, \tag{40}$$

where

$$\rho_i = Zr_i \quad (i = 1, 2, 12). \tag{41}$$

At the limit of $Z \to \infty$, the two-electron atom reduces to two noninteracting H atoms and, therefore, the system total polarizability is equal to the direct summation of those for two H atoms.

Following the asymptotic formula of Drake and Cohen [60] and using Eq. (39), we arrive at the approximate Z-scaling laws for the quantities α, C_6, and C_9 in the forms

$$\lim_{Z\to\infty}(Z - 0.359375)^4\alpha^{\rm He}(Z) = 2\alpha^{\rm H}(Z = 1) = 9, \tag{42}$$

TABLE V. The ground state energy E_0, static dipole polarizability α, two-atom dispersion coefficient C_6, and three-atom dispersion coefficient C_9 for the He-like ions predicted by the VPT method with $k = 15$. All ground state wave functions are represented by the (8,6,4)0 STOCI basis set. Numbers in square brackets represent powers of ten.

Z	E_0	α	C_6	C_9
2	−2.903636	1.379455	1.458424	1.473397
	−2.903724[a]	1.383192[b]	1.460978[b]	1.443[c]
3	−7.279795	1.922553[−1]	7.821339[−2]	1.106324[−2]
	−7.279913[a]	1.924532[−1][b]	7.826431[−2][b]	1.056[−2][c]
4	−1.365543[1]	5.224078[−2]	1.120653[−2]	4.314976[−4]
	−1.365557[1][a]	5.226876[−2][b]	1.121033[−2][b]	3.99[−4][c]
5	−2.203083[1]	1.963781[−2]	2.598519[−3]	3.764680[−5]
	−2.203097[1][a]	1.964429[−2][b]	2.599064[−3][b]	
6	−3.240609[1]	8.961937[−3]	8.041013[−4]	5.319571[−6]
	−3.240625[1][a]	8.963931[−3][b]	8.042154[−4][b]	
7	−4.478129[1]	4.654770[−3]	3.017559[−4]	1.037269[−6]
	−4.478145[1][a]	4.655522[−3][b]	3.017872[−4][b]	
8	−5.915643[1]	2.652184[−3]	1.300197[−4]	2.547274[−7]
	−5.915660[1][a]	2.652507[−3][b]	1.300299[−4][b]	
9	−7.553155[1]	1.620042[−3]	6.215765[−5]	7.440098[−8]
	−7.553171[1][a]	1.620196[−3][b]	6.216146[−5][b]	
10	−9.390664[1]	1.044710[−3]	3.222333[−5]	2.487704[−8]
	−9.390681[1][a]	1.044791[−3][b]	3.222493[−5][b]	
12	−1.366568[2]	4.910669[−4]	1.040106[−5]	3.775374[−9]
	−1.366569[2][a]			
14	−1.874069[2]	2.603092[−4]	4.018668[−6]	7.733737[−10]
	−1.874071[2][a]			
16	−2.461569[2]	1.505462[−4]	1.768916[−6]	1.969024[−10]
	−2.461571[2][a]			
18	−3.129070[2]	9.301118[−5]	8.595623[−7]	5.911935[−11]
	−3.129072[2][a]			
20	−3.876571[2]	6.052045[−5]	4.513812[−7]	2.020212[−11]
	−3.876572[2][a]			

[a]Drake [55].
[b]Zhu *et al.* [56].
[c]Patil [57].

$$\lim_{Z\to\infty}(Z-0.359375)^6 C_6^{\mathrm{He}}(Z) = 4C_6^{\mathrm{H}}(Z=1) = 26, \quad (43)$$

$$\lim_{Z\to\infty}(Z-0.359375)^{10} C_9^{\mathrm{He}}(Z) = 8C_9^{\mathrm{H}}(Z=1) = 173.14. \quad (44)$$

We display in Fig. 4 the variation of α, C_6, and C_9 for the ground state of He-like ions as a function of nuclear charge, on a log-log scale. The good agreement among different theoretical calculations and with the approximate Z-scaling laws indicates that the present development of the VPT method is suitable for extracting the asymptotic behaviors of both the polarizabilities and dispersion coefficients for highly charged ions.

D. Plasma-screened atoms

In this section, we focus on application of the VPT method in the fast calculation of dynamic polarizabilities and dispersion coefficients for atoms embedded in plasma environments. For a large range of distribution of plasmas in the temperature-density diagram (see, e.g., Fig. 1 in Ref. [61]), the weakly coupled classical plasmas with $\Gamma_e < 1$ can be well modeled by the Debye-Hückel model [62], where Γ_e is the electron-electron Coulomb coupling parameter. For one-electron atoms embedded in weakly coupled classical plasmas, the effective Hamiltonian is given by

$$H = -\frac{1}{2}\nabla^2 - Z\frac{e^{-\lambda r}}{r}, \quad (45)$$

where the potential parameter $\lambda = 1/D$ represents the statically averaged screening strength from the plasma electrons. $D = \sqrt{\frac{k_B T_e}{4\pi e^2 n_e}}$ is the well-defined Debye length in which n_e and T_e are, respectively, the plasma electron density and temperature [63]. Following the same model, the Hamiltonian of plasma-screened two-electron atoms is

$$H = -\frac{1}{2}\nabla_1^2 - \frac{1}{2}\nabla_2^2 - Z\frac{e^{-\lambda r_1}}{r_1} - Z\frac{e^{-\lambda r_2}}{r_2} + \frac{e^{-\lambda r_{12}}}{r_{12}}. \quad (46)$$

Here we use the simplified model that the surrounding plasma electrons produce the same screening effect (i.e., same screening parameter λ) on both the electron-nucleus and electron-electron interactions.

In past decades, a large amount of research has been focused on the investigation of atomic structure and spectral properties affected by different plasma environments

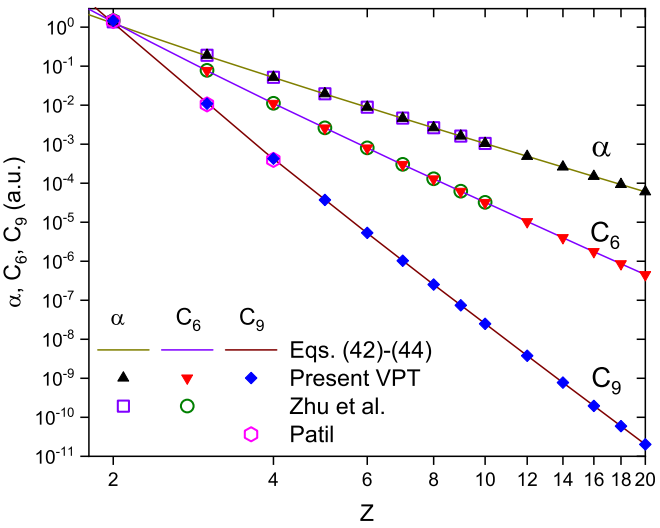

FIG. 4. Static polarizability α and two- and three-atom dispersion coefficients C_6 and C_9 for the ground state of He isoelectronic sequence with $2 \leqslant Z \leqslant 20$. Solid and hollow symbols represent, respectively, the present VPT and previous calculations of Zhu *et al.* [56] and Patil [57]. Solid lines are the approximate Z-scaling laws of Eqs. (42)–(44).

(see Refs. [33–36] for recent reviews). The calculation of dynamic polarizabilities and dispersion coefficients has also attracted considerable interest in the literature [35]. To the best of our knowledge, Kar and Ho [26] first performed accurate predictions of the dispersion coefficients C_6 for H–H, H–He, and He–He interactions under the screening of Debye-Hückel plasmas. Slater-type orbitals and exponentially correlated basis sets were employed for the H and He atoms, respectively, and dispersion coefficients were calculated employing the sum-over-states formalism. Generally speaking, in these sophisticated calculations one needs to optimize both the initial and final states for each screening parameter, and calculate oscillator strengths covering all discrete bound and continuum final states. The present VPT method, which only needs one to optimize the ground state wave function and calculate radial expectation values, provides an alternative, simple, and efficient tool for estimating these quantities.

For the plasma-screened H atom, we employ the numerical GPS method to obtain the ground state wave function for screening parameters that are smaller than the critical value of $\lambda_c^{\mathrm{H}(1s)}$ ($\lambda_c^{\mathrm{H}(1s)} = 1.190612421\ldots$ is defined as the screening parameter beyond which the ground state of the H atom merges into the continuum [64,65]). The present VPT calculations of α, C_6, and C_9 are displayed in Table VI with all results converging to the last reported digit by gradually increasing k. The dipole polarizabilities are in full agreement with our previous sum-over-states calculations [38] over the entire range of λ. The present H-H C_6 coefficients reproduce perfectly the prediction of Kar and Ho [26] for $\lambda < 0.7$, and the H–H–H C_9 coefficients in Debye plasmas are only reported by us.

Figure 5(a) depicts an overview of the variation of α, C_6, and C_9 as a function of screening parameters. All quantities show fast increase as λ approaches λ_c. Such behavior apparently indicates that the system wave function becomes increasingly diffuse when the plasma screening strength is increased. The asymptotic behavior of an atomic system near its critical bound region is of special importance, from both the fundamental and practical aspects, to provide insights to threshold laws and quantum phase transitions [65–68]. As we can see from Fig. 5(b), the three quantities in the critical region follow negative power laws as

$$\alpha^{\mathrm{H}}(\lambda) \propto (\lambda_c - \lambda)^{-4}, \tag{47}$$

TABLE VI. Static dipole polarizability α, two-atom dispersion coefficient C_6, and three-atom dispersion coefficient C_9 for the ground state of the H atom at different values of λ. Numbers in square brackets represent powers of ten.

λ	α	C_6	C_9
0	4.500000000000	6.499026705406	2.164246451064[1]
0.1	4.699777471480	6.912658665498	2.402663529021[1]
0.2	5.276368793394	8.150277486768	3.175222942955[1]
0.3	6.315035521549	1.052505598588[1]	4.895190131737[1]
0.4	8.075794695589	1.492800054106[1]	8.847436269678[1]
0.5	1.114765595284[1]	2.358193377878[1]	1.920176199460[2]
0.6	1.693124176675[1]	4.262824112802[1]	5.240270096428[2]
0.7	2.922556619973[1]	9.239978397486[1]	1.946689821914[3]
0.8	6.061406659843[1]	2.607535300661[2]	1.130710421976[4]
0.9	1.676953145335[2]	1.121290952566[3]	1.336063259043[5]
1.0	7.834765746428[2]	1.050409540798[4]	5.821620802412[6]
1.1	1.354489629424[4]	7.001970015724[5]	6.698805761060[9]
1.12	3.590778714219[4]	2.978988850247[6]	7.55500122387[10]
1.13	6.541410695626[4]	7.272925360853[6]	3.36009835909[11]
1.14	1.330958873464[5]	2.096046127390[7]	1.97030869672[12]
1.15	3.176138469271[5]	7.673455935299[7]	
1.16	9.735291757571[5]	4.089676843279[8]	
1.17	4.686915192955[6]	4.290958447924[9]	
1.18	6.601807271684[7]	2.25324461266[11]	

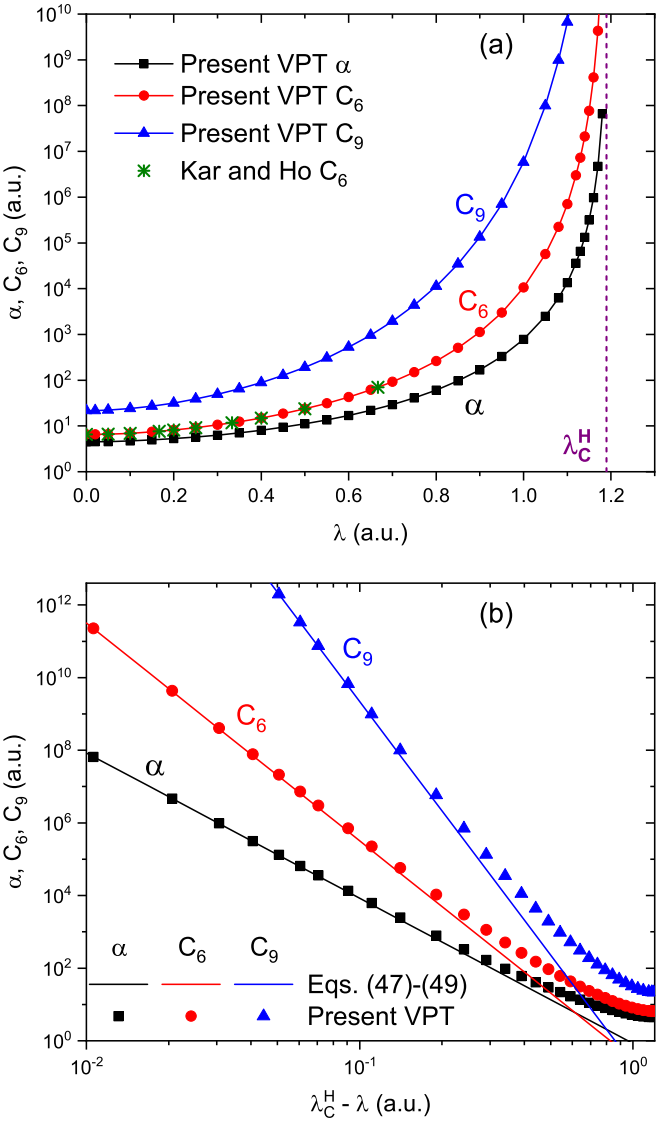

FIG. 5. Static polarizability α and two- and three-atom dispersion coefficients C_6 and C_9 for the ground state of the H atom as a function of (a) λ and (b) $\lambda_c - \lambda$. In panel (a) the vertical line indicates the critical screening parameter λ_c^{H}. The asymptotic laws of Eqs. (47)–(49) are included in panel (b) to guide the eye

$$C_6^{\mathrm{H}}(\lambda) \propto (\lambda_c - \lambda)^{-6}, \tag{48}$$

$$C_9^{\mathrm{H}}(\lambda) \propto (\lambda_c - \lambda)^{-10}. \tag{49}$$

Equation (47) can be conveniently understood from the asymptotic laws of energy and radial expectation values based on the VPT method, e.g., the Kirkwood ($k = 1$) and Buckingham ($k = 2$) approximations [65,66]. Equations (48) and (49) can be derived by analogy to Eq. (39). An interesting comparison can be made between the critical laws of Eqs. (47)–(49) and the approximate Z-scaling laws in Eqs. (42)–(44), where the increase of screening parameter (nuclear charge) systematically extends (contracts) the wave functions into a larger (smaller) region, which results in negative (positive) power laws in corresponding asymptotic region.

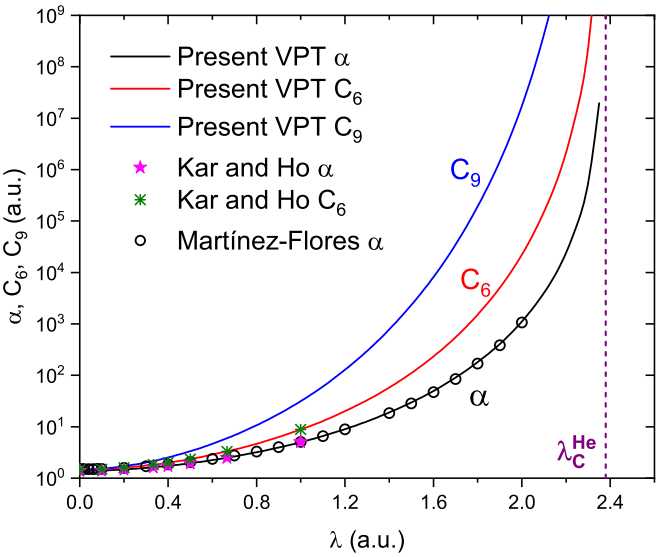

FIG. 6. Static polarizability α and two- and three-atom dispersion coefficients C_6 and C_9 for the ground state of the He atom as a function of screening parameter λ. Solid dots are the referenced calculations from Kar and Ho [26,27]. Open circles represent the dipole polarizabilities from Martínez-Flores and Cabrera-Trujillo [30]. The vertical line indicates the critical screening parameter λ_c^{He}.

The present VPT calculations of α, C_6, and C_9 for the ground state of the He atom are shown in Table VII and depicted in Fig. 6 for a wide range of screening parameters. The similar trends between Figs. 6 and 5(a) demonstrate similar expansion behavior of atoms in the plasma screening environment. Although without rigorous proof, we found in our previous work [69] very strong evidence that the critical screening parameters for two-electron atoms are the same as those for one-electron ions with the same nuclear charge, i.e., $\lambda_c^{\mathrm{He}} = \lambda_c^{\mathrm{He}^+} = 2\lambda_c^{\mathrm{H}} = 2.381224842\ldots$. For screening parameters that are larger than 2.0, we use the (9,7,5)0 STOCI basis set (680 terms) for better convergence. The estimated ground state energies are always slightly higher than the explicitly-correlated-basis calculations of Kar and Ho [70] (except at $\lambda = 2$ where our result converges better), and the dipole polarizabilities and He-He C_6 coefficients are systematically smaller than the accurate values from the same authors [26,27]. The comparison with Lin *et al.* [28] shown in Table VII is more interesting, where those authors employed the sum-over-states method based on extensively large B-spine CI basis sets (∼4000 and 3500 terms for the S- and P-wave states). The present VPT calculations, with significantly less computational effort, show better agreement with the referenced results [27]. The most recent work of Martínez-Flores and Cabrera-Trujillo [30] estimated the dipole polarizabilities for $\lambda \leqslant 2$ using the restricted Hartree-Fock approach. Their results are larger and smaller, respectively, than the present predictions for screening parameters smaller and larger than 1.2. The three-atom dispersion coefficient C_9 for the He atom under Debye plasmas is reported.

Finally, we would like to explore the applicability of the VPT method for real-frequency dynamic polarizabilities of the plasma-screened He atom. Some benchmark results in the

TABLE VII. Ground state energy E_0, static dipole polarizability α, two-atom dispersion coefficient C_6, and three-atom dispersion coefficient C_9 for the ground state of the He atom at different values of λ. All the present results are obtained employing the (8,6,4)0 STOCI basis set, except for $\lambda \geqslant 2$ where the (9,7,5)0 basis set is used. Numbers in square brackets represent powers of ten.

λ	E_0	α	C_6	C_9
0	−2.90364	1.37946	1.45842	1.47340
	−2.90372[a]	1.38319[b]	1.46098[c]	
	−2.90358[c]	1.37785[c]		
	−2.86168[d]	1.48708[d]		
0.05	−2.75646	1.38560	1.46738	1.48890
	−2.75655[a]	1.38936[b]	1.46996[b]	
		1.38393[c]		
0.1	−2.61476	1.40313	1.49309	1.53374
	−2.61485[a]	1.40697[b]	1.49574[b]	
	−2.61471[c]	1.40126[c]		
	−2.57304[d]	1.51062[d]		
0.15	−2.47832	1.43129	1.53471	1.60743
0.2	−2.34692	1.46976	1.59219	1.71151
	−2.34701[a]	1.47383[b]	1.59506[b]	
	−2.34686[c]	1.46681[c]		
	−2.30584[d]	1.57700[d]		
0.25	−2.22038	1.51868	1.66624	1.84952
	−2.22047[a]	1.52294[b]	1.66930[b]	
0.3	−2.09854	1.57857	1.75824	2.02703
	−2.05844[d]	1.68564[d]		
0.4	−1.86836	1.73487	2.00499	2.53572
	−1.86845[a]	1.73995[b]	2.00889[b]	
	−1.82950[d]	1.84458[d]		
0.5	−1.65531	1.94951	2.35853	3.34448
	−1.65540[a]	1.95541[b]	2.36332[b]	
		1.92805[c]		
	−1.61790[d]	2.05526[d]		
0.6	−1.45847	2.24021	2.86250	4.65253
	−1.42268[d]	2.34670[d]		
0.8	−1.11024	3.17528	4.65708	1.0665[1]
	−1.07809[d]	3.26472[d]		
1	−8.1813[−1]	5.00574	8.80735	3.1584[1]
	−8.18214[−1][a]	5.02458[b]	8.83150[b]	
	−7.8997[−1][d]	5.04652[d]		
1.2	−5.7748[−1]	8.97588	2.0047[1]	1.2806[2]
	−5.5357[−1][d]	8.85748[d]		
1.4	−3.8420[−1]	1.8940[1]	5.7979[1]	7.7749[2]
	−3.6471[−1][d]	1.82898[1][d]		
1.6	−2.3455[−1]	4.9752[1]	2.3264[2]	8.1673[3]
	−2.1959[−1][d]	4.70670[1][d]		
1.8	−1.2492[−1]	1.7954[2]	1.5102[3]	1.9114[5]
	−1.1456[−1][d]	1.67900[2][d]		
1.9	−8.3996[−2]	4.0748[2]	5.0414[3]	1.4487[6]
	−7.591[−2][d]	3.82292[2][d]		
2	−5.1743[−2]	1.1117[3]	2.2163[4]	1.7364[7]
	−5.169[−2][a]			
	−4.587[−2][d]	1.05711[3][d]		
2.1	−2.7673[−2]	4.0129[3]	1.4899[5]	4.2151[8]
2.2	−1.1335[−2]	2.4157[4]	2.1680[6]	3.697[10]
2.3	−2.2735[−3]	5.4763[5]	2.3422[8]	9.094[13]

[a]Kar and Ho [70].
[b]Kar and Ho [26,27].
[c]Lin *et al.* [28].
[d]Martínez-Flores and Cabrera-Trujillo [30].

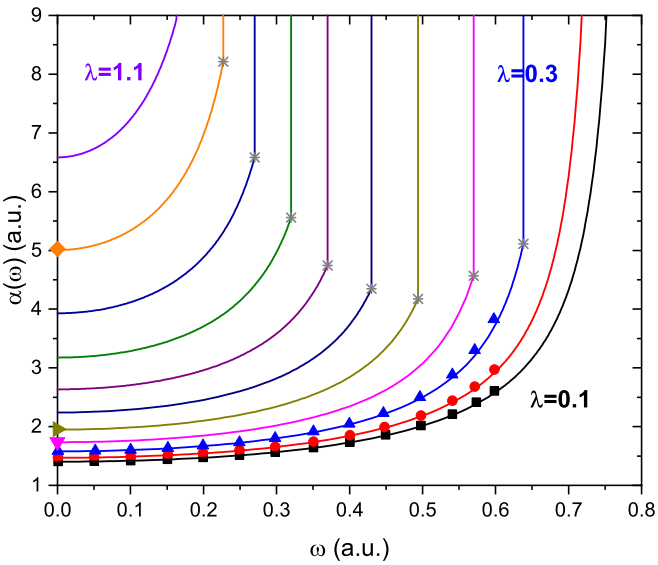

FIG. 7. Real-frequency dynamic polarizability $\alpha(\omega)$ for the ground state of the He atom at screening parameters $\lambda = 0.1$–1.1 (from bottom to top). Solid dots are the referenced values from Kar [29]. Stars indicate the ionization thresholds where the dynamic polarizability ideally goes to infinity.

parameter range of $\lambda \leqslant 0.3$ and $\omega \leqslant 0.6$ are available in the literature for comparison [29]. Our calculations are shown in Fig. 7 for $0.1 \leqslant \lambda \leqslant 1.1$ and all possible values of ω. It is known that the first $^1P^o$ excited state only exists for $\lambda \leqslant 0.21$, beyond which all $^1P^o$-wave bound states are absorbed into the continuum [48]. Therefore, at $\lambda = 0.1$ and 0.2 there exist, respectively, a resonant frequency ω_{r1} at 0.762 and 0.715 [29]. For plasma screening parameters larger than 0.3, the dynamic polarizability increases monotonically from the static quantity and approaches infinity at corresponding λ-dependent ionization threshold $\omega^{\rm He}_{\rm ionization}(\lambda) = E_0^{\rm He^+}(\lambda) - E_0^{\rm He}(\lambda)$. However, since the VPT approximation provides a rigorous lower bound to the exact polarizability, as one can see from comparison with the referenced values shown in Fig. 7, the VPT method is less accurate than the sophisticated sum-over-states method especially near the ionization threshold. For photon frequencies that are smaller than the ionization threshold, the VPT method is expected to be able to produce a good estimate of the behavior of dynamic polarizability.

IV. CONCLUSION

In the present work, we extend the VPT method developed originally for static polarizability to the real- and imaginary-frequency dynamic polarizabilities and the two- and three-atom dispersion coefficients. The present extended VPT method provides the great advantage that only the system ground state wave function and radial expectation values are needed, and at the same time it keeps the feature that it provides rigorous lower bounds to the exact quantities. We tested this method on several one- and two-electron atoms and ions. The converged results for the H atom exactly reproduce the accurate sum-over-states calculations, while for the He atom the VPT method gives a slightly lower estimate of the static

polarizability and dispersion coefficients. We propose that such an underestimate can be further improved by employing more complete basis sets in the orthogonalized subspace. The VPT calculations for the He isoelectronic sequence reveal interesting approximate Z-scaling laws for both polarizabilities and dispersion coefficients.

The recent interest in the spectral properties of atoms embedded in plasma environments requires an increasingly large amount of computational effort to solve the model atoms across a wide range of plasma screening parameters. On the strength of the simplicity and efficiency of the VPT method, we investigated the polarizabilities and dispersion coefficients for the H and He atoms surrounded by weakly coupled plasmas within the Debye-Hückel model. The results for the H atom show asymptotic power laws near the critical bound region which are similar to the inverse of Z-scaling laws in H-like ions. The calculations of static polarizabilities and dispersion coefficients for the plasma-screened He atom show good agreement with the referenced results over a wide range of plasma parameters. The real-frequency dynamic polarizabilities obtained are reasonably accurate for photon frequencies below the resonant and ionization thresholds. Extension of the present work to more complex systems, especially the three-electron atoms, is promising. Due to the fact that the three-electron atoms can be more reasonably treated as hydrogen-like atoms, application of the present VPT method with one-electron excitation approximation to three-electron atoms is probably as good as, or even better than, the situation in two-electron atoms. The introduction of alternative or multielectron excitation basis sets in the orthogonalized subspace is worth trying in the future.

The data that support the findings of this study are available within the article.

ACKNOWLEDGMENTS

This work was supported by the National Natural Science Foundation of China (Grant No. 12174147) and the National Key Research and Development Program of China (Grant No. 2022YFE0134200).

The authors have no conflicts to disclose.

[1] A. Dalgarno, Adv. Phys. **11**, 281 (1962).
[2] D. M. Bishop, Theor. Comput. Chem. **6**, 129 (1999).
[3] J. Mitroy, M. S. Safronova, and C. W. Clark, J. Phys. B: At. Mol. Opt. Phys. **43**, 202001 (2010).
[4] P. Schwerdtfeger and J. K. Nagle, Mol. Phys. **117**, 1200 (2019).
[5] J. G. Kirkwood, Phys. Z. **33**, 57 (1932).
[6] R. A. Buckingham, Proc. R. Soc. Lond. A **160**, 94 (1937).
[7] E. A. Hylleraas, Z. Phys. **65**, 209 (1930).
[8] H. E. Montgomery, Jr. and V. I. Pupyshev, Eur. Phys. J. H **38**, 519 (2013).
[9] H. E. Montgomery, Jr., Eur. J. Phys. **32**, 1275 (2011).
[10] H. E. Montgomery, Jr. and K. D. Sen, Phys. Lett. A **376**, 1992 (2012).
[11] V. I. Pupyshev and H. E. Montgomery, Jr., Int. J. Quantum Chem. **119**, e25887 (2019).
[12] H. E. Montgomery, Jr. and V. I. Pupyshev, Phys. Scr. **95**, 015402 (2020).
[13] A. Kawasaki, Phys. Rev. A **92**, 042507 (2015).
[14] B. M. Henson, R. I. Khakimov, R. G. Dall, K. G. H. Baldwin, L.-Y. Tang, and A. G. Truscott, Phys. Rev. Lett. **115**, 043004 (2015).
[15] J. Kaur, S. Singh, B. Arora, and B. K. Sahoo, Phys. Rev. A **95**, 042501 (2017).
[16] F.-F. Wu, Y.-B. Tang, T.-Y. Shi, and L.-Y. Tang, Phys. Rev. A **100**, 042514 (2019).
[17] A. Dalgarno and W. D. Davision, Adv. At. Mol. Phys. **2**, 1 (1966).
[18] Z.-C. Yan, J. F. Babb, A. Dalgarno, and G. W. F. Drake, Phys. Rev. A **54**, 2824 (1996).
[19] L.-Y. Tang, Z.-C. Yan, T.-Y. Shi, J. F. Babb, and J. Mitroy, J. Chem. Phys. **136**, 104104 (2012).
[20] H. Yang, M.-S. Wu, L.-Y. Tang, M. W. J. Bromley, K. Varga, Z.-C. Yan, and J.-Y. Zhang, J. Chem. Phys. **152**, 124304 (2020).
[21] V. Koch and D. Andrae, Int. J. Quantum Chem. **111**, 891 (2011).
[22] V. Koch and D. Andrae, Eur. Phys. J. D **67**, 139 (2013).
[23] K. Wang, X. Wang, Z. Fan, H.-Y. Zhao, L. Miao, G.-J. Yin, R. Moro, and L. Ma, Eur. Phys. J. D **75**, 46 (2021).
[24] Z.-W. Wang and K. T. Chung, J. Phys. B: At. Mol. Opt. Phys. **27**, 855 (1994).
[25] W. P. Earwood and S. R. Davis, At. Data Nucl. Data Tables **144**, 101490 (2022).
[26] S. Kar and Y. K. Ho, Chem. Phys. Lett. **449**, 246 (2007).
[27] S. Kar and Y. K. Ho, J. Quant. Spectrosc. Radiat. Transfer **109**, 445 (2008).
[28] Y.-C. Lin, C.-Y. Lin, and Y. K. Ho, Phys. Rev. A **85**, 042516 (2012).
[29] S. Kar, Phys. Rev. A **86**, 062516 (2012).
[30] C. Martínez-Flores and R. Cabrera-Trujillo, Eur. Phys. J. D **75**, 133 (2021).
[31] N. Mukherjee, C. N. Patra, and A. K. Roy, Phys. Rev. A **104**, 012803 (2021).
[32] N. Mukherjee, C. N. Patra, and A. K. Roy, Phys. Rev. A **106**, 032812 (2022).
[33] A. N. Sil, S. Canuto, and P. K. Mukherjee, Adv. Quantum Chem. **58**, 115 (2009).
[34] R. K. Janev, S. B. Zhang, and J. G. Wang, Matter Radiat. Extremes **1**, 237 (2016).
[35] S. Kar, Y.-S. Wang, Z. Jiang, Y. Wang, and Y. K. Ho, Chinese J. Phys. **56**, 3085 (2018).
[36] T. A. Gomez, T. Nagayama, P. B. Cho, D. P. Kilcrease, C. J. Fontes, and M. C. Zammit, J. Phys. B: At. Mol. Opt. Phys. **55**, 034002 (2022).
[37] H. A. Bethe and E. E. Salpeter, *Quantum Mechanics of One- and Two-Electron Atoms* (Dover, New York, 2008)
[38] L. Zhu, Y. Y. He, L. G. Jiao, Y. C. Wang, and Y. K. Ho, Phys. Plasmas **27**, 072101 (2020).
[39] Y.-S. Wang, S. Kar, and Y. K. Ho, Int. J. Quantum Chem. **120**, e26115 (2020).
[40] G. Yao and S. I. Chu, Chem. Phys. Lett. **204**, 381 (1993).
[41] S. I. Chu and D. A. Telnov, Phys. Rep. **390**, 1 (2004).

[42] L. Zhu, Y. Y. He, L. G. Jiao, Y. C. Wang, and Y. K. Ho, Int. J. Quantum Chem. **120**, e26245 (2020).
[43] L. G. Jiao, Y. Y. He, Y. Z. Zhang, and Y. K. Ho, J. Phys. B: At. Mol. Opt. Phys. **54**, 065005 (2021).
[44] Y. Y. He, Z. L. Zhou, L. G. Jiao, A. Liu, H. E. Montgomery, Jr., and Y. K. Ho, Phys. Rev. E **107**, 045201 (2023).
[45] M. W. J. Bromley and J. Mitroy, Int. J. Quantum Chem. **107**, 1150 (2007).
[46] G. W. F. Drake, M. M. Cassar, and R. A. Nistor, Phys. Rev. A **65**, 054501 (2002).
[47] K. Pachucki and J. Sapirstein, Phys. Rev. A **63**, 012504 (2000).
[48] L. G. Jiao and Y. K. Ho, Phys. Rev. A **90**, 012521 (2014).
[49] G. W. F. Drake, *Springer Handbook of Atomic, Molecular, and Optical Physics*, edited by G. W. F. Drake (Springer, New York, 2006), Chap. 11, p. 199.
[50] J. S. Sims and S. A. Hagstrom, Int. J. Quantum Chem. **90**, 1600 (2002).
[51] J. S. Sims and S. A. Hagstrom, J. Chem. Phys. **140**, 224312 (2014).
[52] L. G. Jiao, L. R. Zan, L. Zhu, Y. Z. Zhang, and Y. K. Ho, Phys. Rev. A **100**, 022509 (2019).
[53] J. Mitroy, S. Bubin, W. Horiuchi, Y. Suzuki, L. Adamowicz, W. Cencek, K. Szalewicz, J. Komasa, D. Blume, and K. Varga, Rev. Mod. Phys. **85**, 693 (2013).
[54] D. M. Bishop and J. Pipin, Int. J. Quantum Chem. **45**, 349 (1993).
[55] G. W. F. Drake, Energy and wave functions for heliumlike atoms, http://drake.sharcnet.ca/wiki/index.php/Downloadable_Resources.
[56] J.-M. Zhu, B.-L. Zhou, and Z.-C. Yan, Chem. Phys. Lett. **313**, 184 (1999).
[57] S. H. Patil, J. Phys. B: At. Mol. Opt. Phys. **23**, 1 (1990).
[58] Y. Y. Qi, J. G. Wang, and R. K. Janev, Phys. Rev. A **80**, 032502 (2009).
[59] A. Dalgarno and A. L. Stewart, Proc. R. Soc. Lond. A **257**, 534 (1960).
[60] G. W. F. Drake and M. Cohen, J. Chem. Phys. **48**, 1168 (1968).
[61] P. K. Shukla and B. Eliasson, Rev. Mod. Phys. **83**, 885 (2011).
[62] P. Debye and E. Hückel, Z. Phys. **24**, 185 (1923).
[63] J. C. Weisheit and M. S. Murillo, *Springer Handbook of Atomic, Molecular, and Optical Physics*, edited by G. W. F. Drake (Springer, New York, 2006), Chap., p. 1303.
[64] C. G. Diaz, F. M. Fernández, and E. A. Castro, J. Phys. A: Math. Gen. **24**, 2061 (1991).
[65] L. G. Jiao, H. H. Xie, A. Liu, H. E. Montgomery Jr., and Y. K. Ho, J. Phys. B: At. Mol. Opt. Phys. **54**, 175002 (2021).
[66] M. Klaus and B. Simon, Ann. Phys. (NY) **130**, 251 (1980).
[67] J. P. Neirotti, P. Serra, and S. Kais, Phys. Rev. Lett. **79**, 3142 (1997).
[68] S. Kais and P. Serra, in *Advances in Chemical Physics, Vol. 125*, edited by I. Prigogine and S. A. Rice (Wiley, New York, 2003), Chap. 1, p. 1.
[69] X. N. Li, Y. Z. Zhang, L. G. Jiao, Y. C. Wang, H. E. Montgomery Jr., Y. K. Ho, and S. Fritzsche, Eur. Phys. J. D **77**, 96 (2023).
[70] S. Kar and Y. K. Ho, Int. J. Quantum Chem. **106**, 814 (2006).